doi: 10.18323/2782-4039-2024-1-67-8

The influence of tungsten carbide and boride additives on the structure and microhardness of CrFeNi equiatomic coating formed by short-pulse laser cladding

© 2024

Aleksandr K. Stepchenkov*[1,4], junior researcher
Aleksey V. Makarov[1,5], Doctor of Sciences (Engineering), Corresponding member of RAS, Head of Department of Materials Science, Head of Laboratory of Mechanical Properties
Elena G. Volkova[1,6], PhD (Physics and Mathematics), senior researcher
Svetlana Kh. Estemirova[2,7], PhD (Chemistry), senior researcher
Evgeny V. Kharanzhevskiy[3,8], Doctor of Sciences (Engineering), Professor, Head of Laboratory of Physics and Chemistry of Materials
[1]*M.N. Mikheev Institute of Metal Physics of the Ural Branch of RAS, Yekaterinburg (Russia)*
[2]*Institute of Metallurgy of the Ural Branch of RAS, Yekaterinburg (Russia)*
[3]*Udmurt State University, Izhevsk (Russia)*

***E-mail: stepchenkov@imp.uran.ru, alexander.stepchenkov@gmail.com**

[4]ORCID: https://orcid.org/0000-0001-9431-0170
[5]ORCID: https://orcid.org/0000-0002-2228-0643
[6]ORCID: https://orcid.org/0000-0003-4958-3027
[7]ORCID: https://orcid.org/0000-0001-7039-1420
[8]ORCID: https://orcid.org/0000-0002-1525-2169

Received 27.06.2023 *Accepted 30.01.2024*

Abstract: A coating based on a single-phase medium-entropy CrFeNi alloy with a face centered cubic (fcc) structure has good ductility, relatively high anti-corrosion properties, low cost, but insufficient strength for its widespread use. It is assumed that adding strengthening particles in the form of tungsten carbides and borides to the CrFeNi equiatomic coating will lead to an increase in its mechanical properties. This work studies the influence of tungsten carbide and boride additives on the structure and microhardness of a CrFeNi equiatomic coating. The coatings were formed by layer-by-layer short-pulse laser cladding with preplaced powder on a multifunctional laser installation equipped with a solid-state laser with a lamp pump based on an Nd:YAG crystal. The change in phase composition when adding strengthening particles was detected using X-ray diffraction analysis and transmission electron microscopy (TEM). Both methods confirmed the precipitation of $Cr_{23}C_6$ chromium carbide in the deposited coatings. TEM photographs indicate that the precipitated phase is distributed along the grain boundaries of the γ-solid solution. The study found that the addition of 6 wt. % WC and 3 wt. % WB increases the level of microhardness of the CrFeNi coating by 26 % (from 340±6 to 430±12 HV 0.025). This occurs due to the presence of $Cr_{23}C_6$, WC particles in the structure and possible microdistortions of the crystal lattice of the γ-phase as a result of doping with tungsten atoms released during the dissolution of tungsten borides and carbides in the process of high-temperature short-pulse laser heating.

Keywords: CrFeNi coating; medium-entropy alloys; tungsten carbides/borides; short-pulse laser cladding; equiatomic coatings; microhardness.

Acknowledgments: The work was carried out within the state assignment to M.N. Mikheev Institute of Metal Physics of the Ural Branch of the Russian Academy of Sciences (IMP UB RAS) on the topic “Structure” No. 122021000033-2. The research was carried out using the equipment of the Electron Microscopy and Mechanical Testing Departments of the Collaborative Access Center “Testing Center of Nanotechnology and Advanced Materials” of IMP UB RAS.

A.K. Stepchenkov thanks M.N. Mikheev Institute of Metal Physics for the support of the work under the state assignment to IMP UB RAS on the topic “Structure” No. 122021000033-2, which was carried out within the framework of the IMP UB RAS youth project No. 22-13/mol.

The paper was written on the reports of the participants of the XI International School of Physical Materials Science (SPM-2023), Togliatti, September 11–15, 2023.

For citation: Stepchenkov A.K., Makarov A.V., Volkova E.G., Estemirova S.Kh., Kharanzhevskiy E.V. The influence of tungsten carbide and boride additives on the structure and microhardness of CrFeNi equiatomic coating formed by short-pulse laser cladding. *Frontier Materials & Technologies*, 2024, no. 1, pp. 83–94. DOI: 10.18323/2782-4039-2024-1-67-8.

INTRODUCTION

One of the most rapidly developing areas of modern metal science is associated with the development of a new class of materials – high-entropy alloys (HEAs). These alloys appeared relatively recently, in 2004, usually contain at least five elements, and the amount of each of them should not be less than 5 at. % [1; 2]. Due to

significant differences in the processes of structure and phase formation, HEAs are classified as a separate group of materials, that have mechanical and functional properties, as well as thermal stability, different from traditional alloys (the main element as a matrix and a set of alloying elements). As a result, HEAs can have unique strength, tribological and corrosion properties in a wide temperature range [3–5].

Medium-entropy alloys (MEAs) consist of three or more main elements with approximately equal atomic percentages, and their configuration entropy is in the range of 1–1.5 R (R is the universal gas constant) [6]. Due to the high mixing entropy associated with a disordered solution of several elements, both MEAs and HEAs can form stable single-phase solid solutions in which, in an ideal situation, atoms of different sizes are uniformly distributed.

Most industrial equipment is exposed to aggressive external influence, such as high thermal and mechanical loads. To ensure long-term operability, and stability of this equipment, a functional surface layer (coating) with high mechanical, anti-corrosion and other properties is required. It is the surface layers, in which the processes of wear, corrosion, cavitation damage and the initiation of fatigue cracks develop, which are the main reasons for the failure of the bulk of parts and mechanisms. Therefore, the use of expensive HEAs and MEAs, in the form of thin laser coatings, and not in the form of an entirely manufactured part, will provide a significant economic effect due to material saving [7].

At the same time, the technology of laser surfacing, using short-pulse radiation, has a number of significant advantages. These include the possibility of producing a homogeneous, and dense layer of coating material of a specified thickness with a good metallurgical bonding, with the substrate material [8], as well as the possibility of forming nonequilibrium microstructures with unique physical, and mechanical properties [9]. Due to high energy densities, the thermal effect on the substrate is minimized [9; 10]. The continuous development of laser technologies makes them attractive for use, due to relative ease of operation, low cost, and high processing efficiency.

The system of Cr–Fe–Ni components is the basis for a large number of MEAs and HEAs. Taken together, these components form a medium-entropy equiatomic alloy with relatively high anti-corrosion, mechanical and wear-resistant properties, as well as low cost compared to other multicomponent alloys.

Generally, single-phase face centered cubic (fcc) structure HEAs and MEAs have good ductility, but low strength [11]. Therefore, the development of ways to improve the mechanical properties of these alloys is an up-to-date area for further research. The strength of multicomponent alloys can be increased through solid solution strengthening, by adding elements with a large atomic radius. The second phase precipitation in the fcc matrix can also improve the mechanical properties of the alloy [12].

To increase the hardness of traditional alloys, additives of various strengthening particles are used – carbides, borides, etc. Tungsten carbide WC is well known for its high hardness, high chemical stability and oxidation resistance, which makes it possible to use it as a reinforcing phase in composite coatings to increase wear resistance [13–15]. It is known that tungsten borides have good chemical inertness, high wear resistance and hardness, as well as a high fusion temperature [16; 17]. Based on this, it can be assumed that the addition of strengthening particles in the form of tungsten carbides and borides during short-pulse laser cladding of the CrFeNi alloy can be an effective way to increase its strength characteristics.

The purpose of this work is to study changes in the structural-phase state and microhardness of a coating based on an equiatomic CrFeNi alloy, formed by short-pulse laser cladding with the addition of tungsten carbides and borides.

METHODS

Multicomponent coatings, based on medium-entropy alloys, were formed by layer-by-layer short-pulse laser cladding, with preplaced powder on a LRS AU multifunctional laser system (manufactured by the "OKB BULAT"), equipped with a solid-state Nd:YAG laser (wavelength is 1.065 μm).

The substrate material, was plates of AISI 1035 (chemical composition: Fe–C0.38–Si0.34–Mn0.65–Cr0.13–Ni0.06–Cu0.09 wt. %; as-delivered state), with dimensions of 45×45×10 mm^3. Before applying the coating, the surface of the plates was cleaned from oxides using sandpaper. As the base coating material, an equiatomic alloy of the Cr–Fe–Ni system was used in the form of a spherical powder, with a fraction of 50–150 μm (supplied by PJSC "Ashinsky Metallurgical Plant", Asha, Russia), the chemical composition of which is given in Table 1. To strengthen the CrFeNi matrix of the coating, GP10BN powder (60 % WC + 30 % WB + 10 % Co) with the fraction of 10–30 μm was used produced by Luoyang Golden Egret Geotools Co., Ltd (China). The surfacing material of the multicomponent coating was obtained by mechanically mixing CrFeNi alloy powder, and the GP10BN powder in amounts of 3 and 10 wt. %. Consequently, CrFeNi + 1.8 % WC + 0.9 % WB + 0.3 % Co and CrFeNi + 6 % WC + 3 % WB + 1 % Co coatings were obtained (wt. %). A coating without adding the alloying elements (CrFeNi), acted as a base coating to compare the resulting structural features and micromechanical properties.

Laser cladding with preplaced powder was used to apply the coating. A preplaced layer of the material was produced by applying a suspension (10 g of a mixture of CrFeNi powder and alloying additive (GP10BN powder); 2 ml of alcohol-rosin solution) and subsequent levelling with a special device ("knife") to achieve a uniform thickness (~200 μm) of the layer over the entire deposited area. Then, the plate with the applied layer of suspension was dried with a heat gun for 15–20 s. After this, the plate was placed in a chamber with continuous inert gas (argon) purging. Laser scanning of the deposited layer of the material was carried out according to the scheme shown in Fig. 1 a.

The following laser cladding parameters were used: pulse duration – 3.5 ms; pulse frequency – 20 Hz; pulse energy – 8.3 J; distance between scanning lines – 0.8 mm;

Table 1. *Chemical composition of CrFeNi powder, wt. %*
Таблица 1. *Химический состав порошка CrFeNi, мас. %*

Fe	Ni	Cr	C	S	P	Si
Base	35.6	29.8	0.37	<0.001	0.008	1.62

the diameter of the laser spot in the focal plane was ~1 mm. After this, the deposited coating was re-exposed to laser action, but with a greater degree of laser defocusing in order to obtain a surface with less roughness. To reduce the effect of mixing the coating material with the substrate material, the coating was applied in three layers.

Measurements of Vickers microhardness (HV) of coatings, as well as the construction of 2*D* maps of its distribution, were carried out on a cross-section using a Q10A+ automated microhardness tester (Qness, Austria). The load on the Vickers indenter was 0.245 N (25 gf), and the holding time was 10 s. The measurement error was determined by the standard deviation with a confidence level of p=0.95. The presence of an optical system, with magnifying lenses, made it possible to use this equipment for studying the macrostructure.

X-ray diffraction analysis (XRD) was performed using a XRD-7000 diffractometer (Shimadzu, Japan) in Cu–K_α radiation, using a graphite monochromator. X-ray tube voltage U=40 kV, current I=30 mA, focus size 1×10 mm^2, external standard is silicon powder. The diffraction spectrum was recorded in the angular range of 2Θ=30–120°, in a step-by-step mode with a scanning step of Δθ=0.03° and a pulse accumulation duration of 2 s. Phase identification was carried out using the PDF-2 database of the International Centre for Diffraction Data (ICDD). The ICDD data bank also contains a program of quantitative analysis using the corundum number method, which was applied to determine the relative content of the phases. Corundum numbers (the ratio of the intensities of the maximum lines of phases, and the reference phase of corundum (α-Al_2O_3) in a 1:1 mixture), are accumulated in the ICDD data bank along with X-ray phase standards. This method is a semi-quantitative estimation.

Measurements of the half-width (full width at half maximum) of diffraction lines, were performed using the "New_profile" software package (free distribution). The package includes a set of means for preliminary processing of diffraction spectra, (background separation, elimination of the $K\alpha_2$ component of the doublet). Background separation was carried out using the least squares method (LSM); to determine the single maxima parameters, the Lorentz quadratic function was used. The software package uses the residual value as a criterion for the quality of fitting. In the process of fitting the Lorentz function to the experimental profiles of single maxima, data on the position of these maxima were obtained, which were then used to calculate the elementary cell parameters of the detected phases.

Since the X-ray diffraction spectrum contained broadened diffraction maxima, we analysed the line broadening using the Williamson–Hall method, which assumes that the broadening is caused by the small sizes of coherent scattering regions (CSR) and microdistortions (ε) of crystalline structure (type II residual stress). The method is based on the following relation:

$$\beta = 4 \cdot \varepsilon \cdot \tan\Theta + \frac{\lambda}{D \cdot \cos\Theta},$$

where β is the physical broadening, rad.;
ε is an average value of microstrains (dimensionless value);
Θ is Bragg angle;
λ is the radiation wavelength (for Cu–K_α λ=1.54051 Å);
D is the CSR size, nm.

Electron microscopy studies were carried out using a JEM-200CX transmission electron microscope (JEOL, Japan). Samples (~300 μm thick) for the production of thin foils were cut out on an electric spark machine, followed by grinding to a thickness of 50–70 μm. Then, they were subjected to double-sided thinning by electropolishing.

RESULTS

Fig. 2 shows a cross-section of a CrFeNi + 6 % WC + + 3 % WB + 1 % Co (wt. %) medium-entropy alloy coating obtained by optical microscopy. As can be seen, the coating thickness value after three-layer laser cladding varies from approximately 620 to 710 μm. The macrostructure of the studied sample shown in Fig. 2 confirms that during the laser cladding, a relatively dense, uniform coating is formed without large defects in the form of cracks. The coating contains isolated continuity defects in the form of pores, which are predominantly round-shaped. It is also worth noting that during laser cladding, an almost defect-free transition zone was formed, between the coating material and the substrate material: there are no peelings of the coating, only isolated elongated pores are observed.

The Vickers microhardness test results indicate an increase in the microhardness of coatings up to 26 %, with the addition of strengthening additives in the form of tungsten carbides and borides. As can be seen from Table 2 and the graph presented in Fig. 3, the average microhardness of the CrFeNi coating formed by laser cladding is 340±6 HV 0.025.

An increase in the mass fraction of WC and WB in coatings, leads to an increase in the microhardness level. The average microhardness level of the CrFeNi + 1.8 % WC + + 0.9 % WB + 0.3 % Co sample is approximately 380±11 HV 0.025, while this feature for the CrFeNi + + 6 % WC + 3 % WB + 1 % Co sample is 430±12 HV 0.025, which is 12 and 26 %, respectively, higher than that of the original sample without strengthening additives.

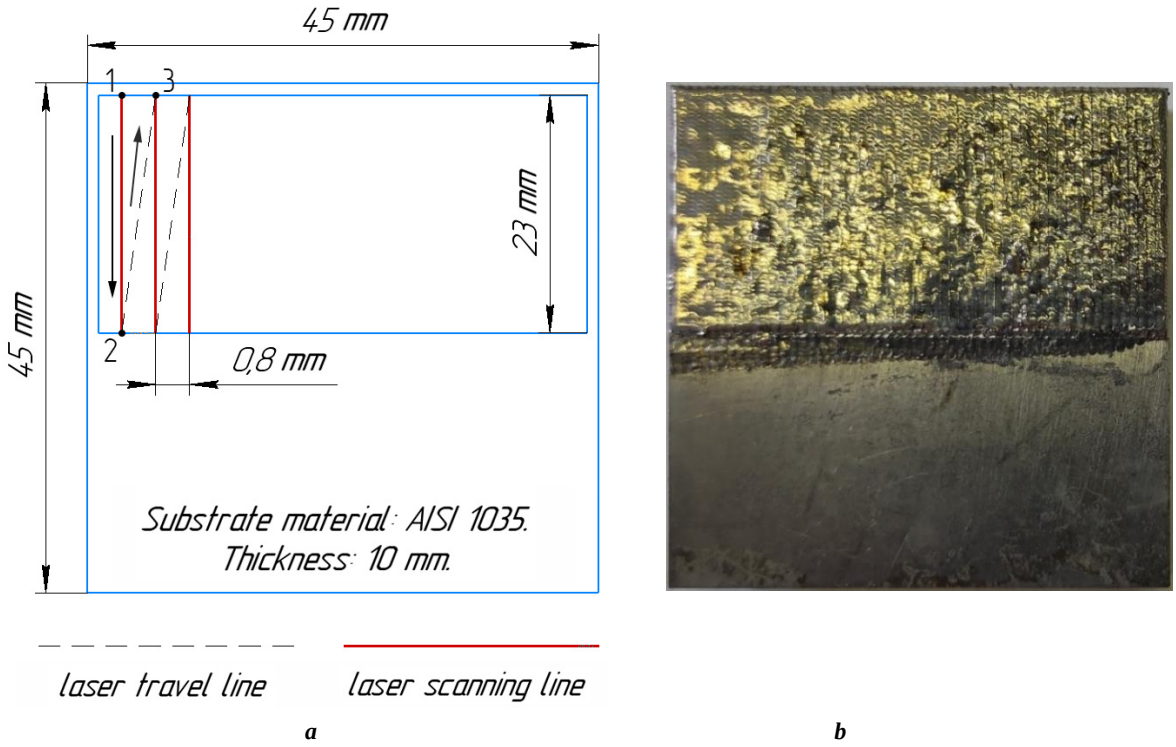

Fig. 1. *Scheme of laser scanning of pre-applied powder (**a**) and appearance of a steel sample with a fused coating (**b**)*
Рис. 1. *Схема лазерного сканирования предварительно нанесенного порошка (**a**) и внешний вид стального образца с наплавленным покрытием (**b**)*

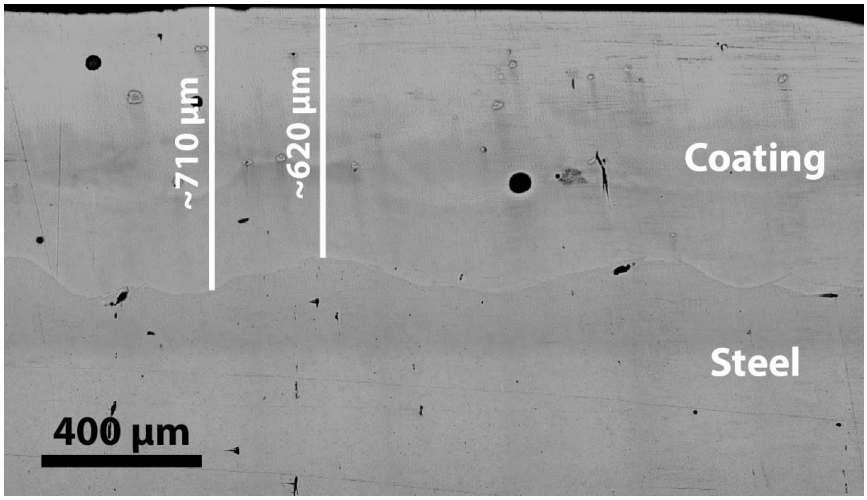

Fig. 2. *Macrostructure of a fused coating based on CrFeNi + 6 % WC + 3 % WB + 1 % Co medium-entropy alloy in the cross-section plane*
Рис. 2. *Макроструктура наплавленного покрытия на основе среднеэнтропийного сплава CrFeNi + 6 % WC + 3 % WB + 1 % Co в плоскости поперечного сечения*

Fig. 4 shows 2D maps of microhardness distribution in the cross-sectional plane of the studied samples, where areas with high microhardness values (465–500 HV 0.025 and above) are marked in red, and areas with the lowest microhardness values (150–200 HV 0.025) are marked in blue. As can be seen, the CrFeNi sample is characterised by a relatively uniform microhardness distribution, in the cross-sectional plane (Fig. 4 a). Slight deviations in the microhardness distribution are observed in the CrFeNi + 1.8 % WC + + 0.9 % WB + 0.3 % Co coating (Fig. 4 b): areas of the coating near the "coating – steel" transition zone have a slightly higher microhardness level.

Fig. 5 presents the XRD results for the CrFeNi + + 6 % WC + 3 % WB + 1 % Co sample. Phase analysis showed, that the sample contains three phases: γ-phase (CrFeNi-based solid solution), chromium carbide $Cr_{23}C_6$

Table 2. *The results of measuring microhardness of the studied samples*
Таблица 2. *Результаты измерения микротвердости исследованных образцов*

Coating	Average value, HV	RMS deviation σ, HV	Range *R*, HV	Coefficient of variation V_σ, %
CrFeNi	340±6	37	175	10.6
CrFeNi + 1.8 % WC + + 0.9 % WB + 0.3 % Co	380±11	51	263	13.4
CrFeNi + 6 % WC + + 3 % WB + 1 % Co	430±12	61	328	14.2

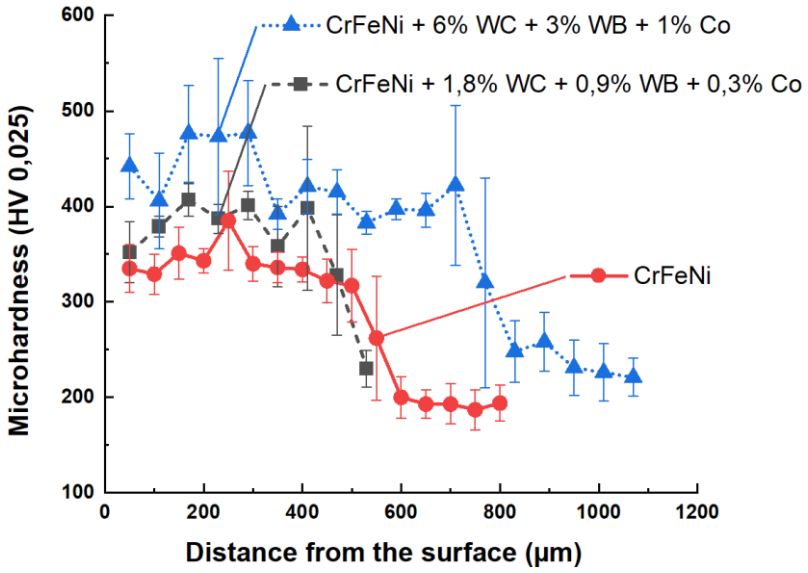

Fig. 3. *Graph of changes in microhardness of samples with deposited coatings depending on the distance from the surface*
Рис. 3. *График изменения микротвердости образцов с наплавленными покрытиями в зависимости от расстояния от поверхности*

(Fm-3m space group), and WC tungsten carbide. The ratio of the diffraction maxima indicates that the γ-phase has a distinct texture with the [200] zone axis. Analysis of the diffraction peak profiles, showed that their width significantly exceeds the instrumental width. As a result of the calculations, it was found that the average size of the γ-phase CSR is 59 nm, and the average value of microstrains (<ε>) was 0.26 %.

The elementary cell parameters calculated using the least squares method (RTP 32 programme), and the quantitative composition are shown in Table 3. It can be observed that the lattice parameter of the CrFeNi-based γ-solid solution practically did not change, when adding the tungsten carbides and borides (a=3.598 Å and a=3.599 Å, respectively). The presented quantitative analysis results for the CrFeNi + 6 % WC + 3 % WB + 1 % Co coating (~86 wt. % of γ, ~13 wt. % of $Cr_{23}C_6$, ~1 wt. % of WC), are estimating due to the presence of the γ-phase crystallite texture.

The TEM method was used to study the structure of a CrFeNi alloy formed by short-pulse laser cladding. Fig. 6 a, 6 b show the sample microstructure features. Elongated subgrains are observed, inside of which there are individual dislocations or dislocation cells. The subgrain boundaries are wide, consisting of clusters of dislocations. The reflections in the microdiffraction image (Fig. 6 a) belong only to the γ-phase, which is also confirmed by the obtained results in [18; 19]. In general, the sample structure is characteristic of samples obtained by selective laser melting and is single-phase.

Fig. 7 shows the structural features of the CrFeNi + + 6 % WC + 3 % WB + 1 % Co sample. In Fig. 7 a, 7 c, fcc grains of 1–2 μm in size, with an elongated or rounded shape are visible. There are a small number of dislocations inside the grains. The $Me_{23}C_6$ phase precipitated along the grain boundaries. In the microdiffraction patterns, except for the fcc reflections of the solid solution, there is a network of $Me_{23}C_6$ reflections (Fig. 7 b). In the dark-field image (Fig. 7 d), precipitates of the $Me_{23}C_6$ phase glow along the grain boundaries.

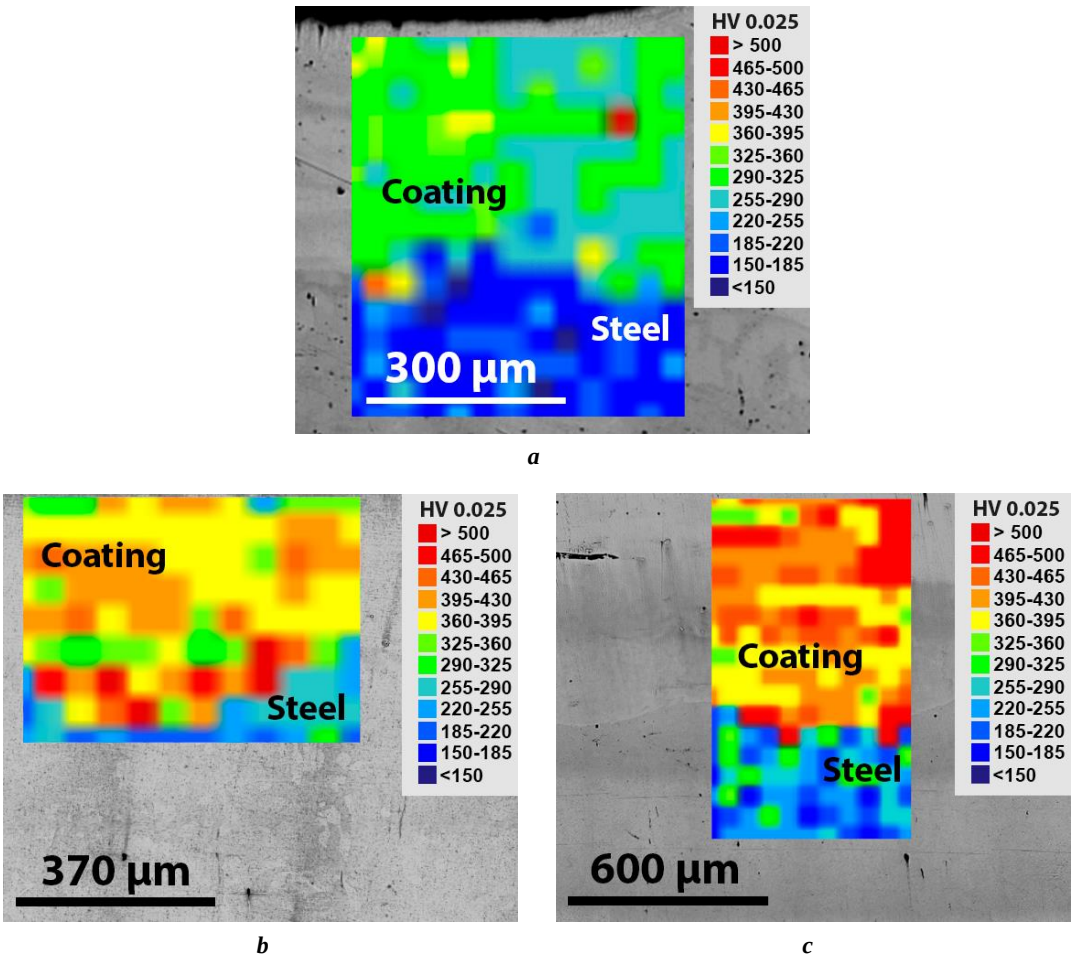

Fig. 4. *2D distribution maps of microhardness of deposited coatings in the cross-sectional plane of the samples:* ***a*** *– CrFeNi;* ***b*** *– CrFeNi + 1.8 % WC + 0.9 % WB + 0.3 % Co;* ***c*** *– CrFeNi + 6 % WC + 3 % WB + 1 % Co*

Рис. 4. *2D-карты распределения микротвердости наплавленных покрытий в плоскости поперечного сечения образцов:* ***a*** *– CrFeNi;* ***b*** *– CrFeNi + 1,8 % WC + 0,9 % WB + 0,3 % Co;* ***c*** *– CrFeNi + 6 % WC + 3 % WB + 1 % Co*

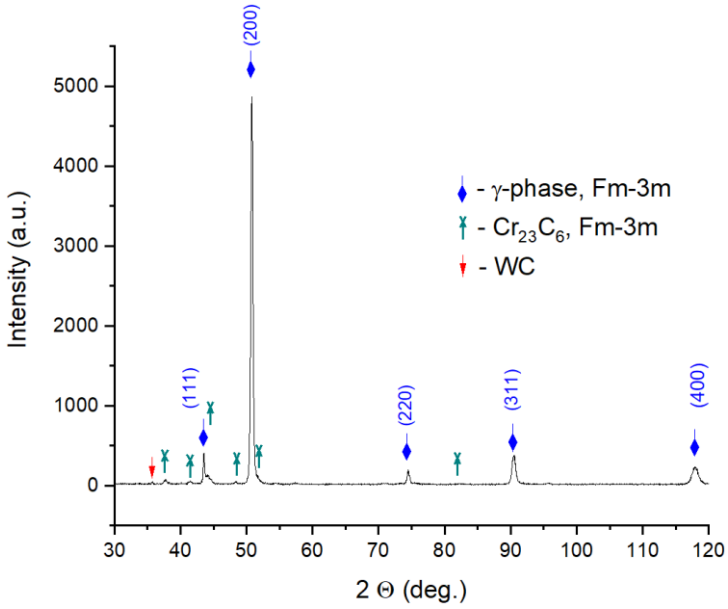

Fig. 5. *X-ray diffraction pattern of the CrFeNi + 6 % WC + 3 % WB + 1 % Co sample*

Рис. 5. *Рентгеновская дифрактограмма образца CrFeNi + 6 % WC + 3 % WB + 1 % Co*

Table 3. *Phase composition, elementary cell parameters of the studied samples*
Таблица 3. *Фазовый состав, параметры элементарной ячейки исследованных образцов*

Phase	Content, wt. %	Elementary cell parameters, Å	
		a	V
CrFeNi coating			
γ-phase, Fm-3m	100.0	3.598	46.58
CrFeNi + 6 % WC + 3 % WB + 1 % Co coating			
γ-phase, Fm-3m	86.2	3.599	46.62
$Cr_{23}C_6$, Fm-3m	12.7	10.660	1 214.20
WC	1.0	–	–

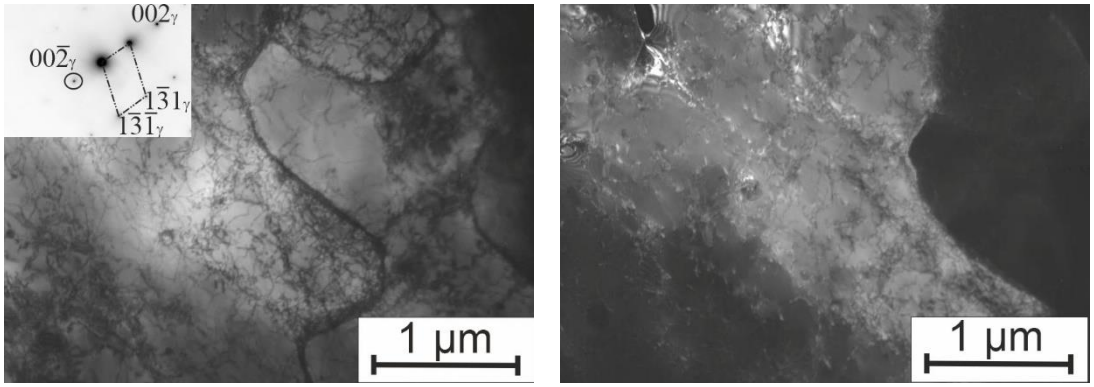

a ***b***

Fig. 6. *Structure of the CrFeNi sample:*
a *– bright-field image; in the insert – microdiffraction pattern, [130]$_\gamma$ zone axis;*
b *– dark-field image in the $00\bar{2}_\gamma$ reflection*

Рис. 6. *Структура образца CrFeNi:*
a *– светлопольное изображение; на вкладке – картина микродифракции, ось зоны [130]$_\gamma$;*
b *– темнопольное изображение в рефлексе $00\bar{2}_\gamma$*

DISCUSSION

It is important to emphasise that the results of this work confirm the fundamental possibility of using a CrFeNi equiatomic alloy as a surface layer formed by laser cladding. This allows saving expensive material. Moreover, to produce a dense coating and a transition zone (from the coating to the steel substrate), without continuity defects (pores), a more careful selection of surfacing technological modes is apparently required.

The microhardness of the CrFeNi alloy depends on the manufacturing technology. For comparison, technologies for producing CrFeNi alloy, not using laser radiation, are characterised by lower microhardness values. Thus, in [18], the CrFeNi alloy produced by the spark plasma sintering technology had an average microhardness of 267 HV. The microhardness of CrFeNi samples produced by vacuum-arc melting in an argon atmosphere was approximately 200 HV [19], while the microhardness of the CrFeNi coating formed by laser cladding is on average 340±6 HV 0.025.

During this work, it was identified that the addition of tungsten carbides and borides has a positive influence on the microhardness values of deposited coatings. A similar approach, to increasing the strength properties of a CrFeNi alloy by adding particles, is mentioned in [20]: adding 1 wt. % of yttrium oxide Y_2O_3 and 1 wt. % of zirconium Zr to the CrFeNi alloy, leads to an increase in microhardness to 474 HV.

Based on the results of the study of the structure and phase composition, one can assume that this strengthening effect is caused by the precipitates of special $Cr_{23}C_6$ chromium carbide formed along the grain boundaries of the γ-solid solution. The hardness of $Cr_{23}C_6$ carbide is 1000–1150 HV [21]. The X-ray method did not reveal the presence of WB tungsten borides in the deposited coating, which in an amount of 3 wt. % was added to the CrFeNi equiatomic alloy powder. However, the XRD method identified a small amount (1 wt. %) of WC tungsten carbide in the coating (Fig. 5, Table 3), which, along with chromium

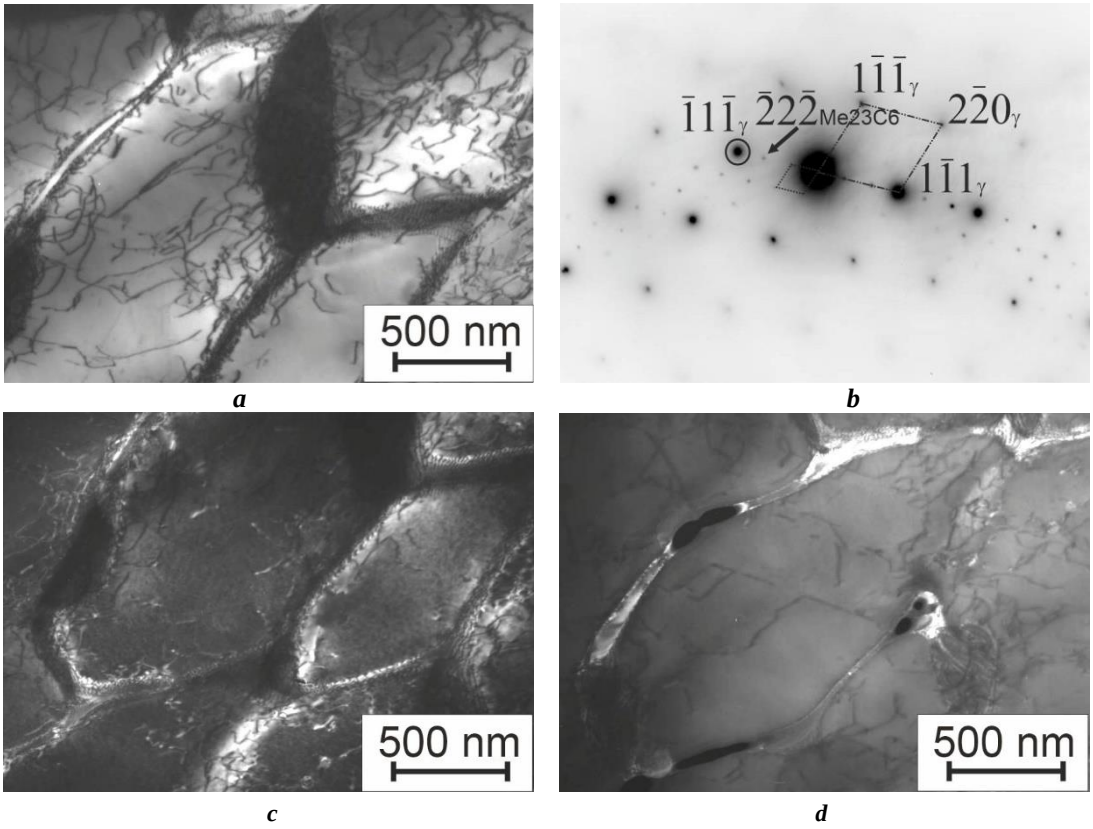

a *b*

c *d*

Fig. 7. *Structure of the CrFeNi + 6 % WC + 3 % WB + 1 % Co sample:*
a *– bright-field image;* ***b*** *– microdiffraction pattern, axis of* $[110]_\gamma$ *and* $[110]_{Me_{23}C_6}$ *zones;*
c *– dark-field image in the* $\bar{1}1\bar{1}_\gamma$ *reflection;* ***d*** *– dark-field image in the* $\bar{2}\bar{2}_{Me_{23}C_6}$ *reflection*

Рис. 7. *Структура образца CrFeNi + 6 % WC + 3 % WB + 1 % Co:*
a *– светлопольное изображение;* ***b*** *– картина микродифракции, оси зон* $[110]_\gamma$ *и* $[110]_{Me_{23}C_6}$ *;*
c *– темнопольное изображение в рефлексе* $\bar{1}1\bar{1}_\gamma$ *;* ***d*** *– темнопольное изображение в рефлексе* $\bar{2}\bar{2}_{Me_{23}C_6}$

carbides, causes dispersion strengthening of the coating. From these data, it follows that tungsten boride completely dissolved during laser cladding of the coating, and tungsten carbide dissolved only partially. This is facilitated by the larger amount of added WC carbide (6 wt. %), as well as the higher melting point of tungsten carbide ($Tmelt_{WC}$=2870 °C), than that of tungsten boride ($Tmelt_{WB}$=2660 °C).

To form $Cr_{23}C_6$ chromium carbide, the presence of free carbon is necessary. Despite the fact that the CrFeNi powder for surfacing contains 0.37 wt. % of C, when surfacing the CrFeNi coating without additives, a single-phase structure of a γ-solid solution is formed. Precipitates of $Cr_{23}C_6$ chromium carbide were found only in coatings with additives. This may lead to the assumption, that part of the WC tungsten carbides (possibly significant) dissolved due to high instantaneous power values during the process of short-pulse laser cladding. In addition, during the crystallization process, carbon formed compounds with chromium, as a more active chemical element.

When WC and WB particles dissolve, as a result of laser cladding, tungsten atoms move into a γ-solid solution based on the Cr–Fe–Ni alloying system, replacing individual chromium, iron or nickel atoms at the crystal lattice sites. This leads to microdistortions of the lattice and corresponding additional coating strengthening.

CONCLUSIONS

This study demonstrated the fundamental possibility of producing relatively high-quality coatings (with the presence of isolated pores) based on a CrFeNi equiatomic alloy with a thickness of 600–700 μm using short-pulse laser cladding with preplaced powder.

TEM method identified that the coating formed from the CrFeNi alloy without strengthening additives using short-pulse laser cladding, is characterised by a single-phase structure (γ-solid solution), with a grain size of 1–2 μm. The addition of strengthening particles in the form of tungsten carbides and borides (WC and WB) to the CrFeNi matrix, leads to the $Me_{23}C_6$ second phase precipitation in the laser coating along the grain boundaries. The results of X-ray diffraction phase analysis confirm the presence of the $Cr_{23}C_6$ phase, in the CrFeNi + 6 % WC+3 % WB + + 1 % Co coating, complete dissolution of WB boride and partial dissolution of WC carbide during laser cladding. According to approximate calculations (due to the presence of texture in the γ-phase), the content of the $Cr_{23}C_6$ phase

precipitated during crystallization is 12.7 wt. %. The elementary cell parameter of the γ-phase does not change significantly, when adding strengthening particles to the CrFeNi-based coating. In both cases it is (3.598–3.599) Å.

The results of Vickers microhardness test indicate that the microhardness in the cross-sectional plane of the samples is characterised by relative homogeneity. Only in the CrFeNi + 6 % WC + 3 % WB + 1 % Co coating, individual areas with an increased microhardness level are observed. The obtained results indicate the strengthening of CrFeNi-based coatings by adding tungsten carbides and borides. The CrFeNi + 1.8 % WC + 0.9 % WB + 0.3 % Co sample has an average microhardness of 380±11 HV 0.025, which is 12 % higher than the initial value. The average microhardness of the CrFeNi + 6 % WC + 3 % WB + 1 % Co sample is 430±12 HV 0.025, which is 26 % higher than the average microhardness level of the CrFeNi coating (340±6 HV 0.025) without strengthening additives.

The strengthening of the CrFeNi + 6 % WC + 3 % WB + + 1 % Co coating is caused by the presence of chromium carbides ($Cr_{23}C_6$), and tungsten carbides (WC) particles in the laser coating structure, as well as, apparently, the occurrence of microdistortions of the crystalline lattice of the γ-solid CrFeNi-based solution due to its doping with tungsten atoms precipitated during the dissolution of tungsten borides, and carbides in the process of high-temperature short-pulse laser heating.

REFERENCES

1. Cantor B., Chang I.T.H., Knight P., Vincent A.J.B. Microstructural development in equiatomic multicomponent alloys. *Materials Science and Engineering: A*, 2004, vol. 375-377, pp. 213–218. DOI: 10.1016/j.msea.2003.10.257.
2. Yeh Jien-Wei, Lin Su-Jien, Chin Tsung-Shune, Gan Jon-Yiew, Chen Swe-Kai, Shun Tao-Tsung, Tsau Chung-Huei, Chou Shou-Yi. Formation of simple crystal structures in Cu–Co–Ni–Cr–Al–Fe–Ti–V alloys with multiprincipal metallic elements. *Metallurgical and Materials Transactions A*, 2004, vol. 35, pp. 2533–2536. DOI: 10.1007/s11661-006-0234-4.
3. Zhang Yong, Zuo Ting Ting, Tang Zhi, Gao M.C., Dahmen K.A., Liaw P.K., Lu Zhao Ping. Microstructures and properties of high-entropy alloys. *Progress in Materials Science*, 2014, vol. 61, pp. 1–93. DOI: 10.1016/j.pmatsci.2013.10.001.
4. Butler T.M., Weaver M.L. Influence of annealing on the microstructures and oxidation behaviors of $Al_8(CoCrFeNi)_{92}$, $Al1_5(CoCrFeNi)_{85}$, and $Al_{30}(CoCrFeNi)_{70}$ high-entropy alloys. *Metals*, 2016, vol. 6, no. 9, article number 222. DOI: 10.3390/met6090222.
5. Daoud H.M., Manzoni A.M., Völkl R., Wanderka N., Glatzel U. Oxidation behavior of $Al_8Co_{17}Cr_{17}Cu_8Fe_{17}Ni_{33}$, $Al_{23}Co_{15}Cr_{23}Cu_8Fe_{15}Ni_{15}$, and $Al_{17}Co_{17}Cr_{17}Cu_{17}Fe_{17}Ni_{17}$ compositionally complex alloys (high-entropy alloys) at elevated temperatures in air. *Advanced Engineering Materials*, 2015, vol. 17, no. 8, pp. 1134–1141. DOI: 10.1002/adem.201500179.
6. Gludovatz B., Hohenwarter A., Thurston K.V.S., Bei Hongbin, Wu Zhenggang, George E.P., Ritchie R.O. Exceptional damage-tolerance of a medium-entropy alloy CrCoNi at cryogenic temperatures. *Nature Communications*, 2016, vol. 7, article number 10602. DOI: 10.1038/ncomms10602.
7. Arif Z.U., Khalid M.Y., Rashid A.A., Rehman E.U., Atif M. Laser deposition of high-entropy alloys: A comprehensive review. *Optics & Laser Technology*, 2022, vol. 145, article number 107447. DOI: 10.1016/j.optlastec.2021.107447.
8. Xiang Kang, Chai Linjiang, Wang Yueyuan, Wang Hao, Guo Ning, Ma Yanlong, Murty K.L. Microstructural characteristics and hardness of CoNiTi medium-entropy alloy coating on pure Ti substrate prepared by pulsed laser cladding. *Journal of Alloys and Compounds*, 2020, vol. 849, article number 156704. DOI: 10.1016/j.jallcom.2020.156704.
9. Geng Yanfei, Konovalov S.V., Chen Xizhang. Research status and application of the high-entropy and traditional alloys fabricated via the laser cladding. *Progress in Physics of Metals*, 2020, vol. 21, no. 1, pp. 26–45. DOI: 10.15407/ufm.21.01.026.
10. Juan Yongfei, Zhang Jiao, Dai Yongbing, Dong Qing, Han Yanfeng. Designing rules of laser-clad high-entropy alloy coatings with simple solid solution phases. *Acta Metallurgica Sinica (English Letters)*, 2020, vol. 33, pp. 1064–1076. DOI: 10.1007/s40195-020-01040-0.
11. Chen Zhao, Wen Xiaoli, Wang Weili, Lin Xin, Yang Haiou, Jiang Ze, Chen Lianyang, Wu Haibin, Li Wenhui, Li Nan. Engineering fine grains, dislocations and precipitates for enhancing the strength of TiB_2-modified CoCrFeMnNi high-entropy alloy using Laser Powder Bed Fusion. *Journal of Materials Research and Technology*, 2023, vol. 26, pp. 1198–1213. DOI: 10.1016/j.jmrt.2023.07.244.
12. He Junyang, Makineni S.K., Lu Wenjun, Shang Yuanyuan, Lu Zhaoping, Li Zhiming, Gault B. On the formation of hierarchical microstructure in a Mo-doped NiCoCr medium-entropy alloy with enhanced strength-ductility synergy. *Scripta Materialia*, 2020, vol. 175, pp. 1–6. DOI: 10.1016/j.scriptamat.2019.08.036.
13. Ren Mengfei, Li Ruifen, Zhang Xiaoqiang, Gu Jiayang, Jiao Chen. Effect of WC particles preparation method on microstructure and properties of laser cladded Ni60-WC coatings. *Journal of Materials Research and Technology*, 2023, vol. 22, pp. 605–616. DOI: 10.1016/j.jmrt.2022.11.120.
14. Cao Qizheng, Fan Li, Chen Haiyan, Hou Yue, Dong Lihua, Ni Zhiwei. Wear behavior of laser cladded WC-reinforced Ni-based coatings under low temperature. *Tribology International*, 2022, vol. 176, article number 107939. DOI: 10.1016/j.triboint.2022.107939.
15. Sabzi M., Dezfuli S.M., Mirsaeedghazi S.M. The effect of pulse-reverse electroplating bath temperature on the wear/corrosion response of Ni-Co/tungsten carbide nanocomposite coating during layer deposition. *Ceramics International*, 2018, vol. 44, no. 16, pp. 19492–19504. DOI: 10.1016/j.ceramint.2018.07.189.
16. Dash T., Nayak B.B. Preparation of multi-phase composite of tungsten carbide, tungsten boride and carbon by arc plasma melting: characterization of melt-cast product. *Ceramics International*, 2016, vol. 42, no. 1-A, pp. 445–459. DOI: 10.1016/j.ceramint.2015.08.129.

17. Chen Hai-Hua, Bi Yan, Cheng Yan, Ji Guangfu, Peng Fang, Hu Yan-Fei. Structural and thermodynamic properties of WB at high pressure and high temperature. *Physica B: Condensed Matter*, 2012, vol. 407, no. 24, pp. 4760–4764. DOI: 10.1016/j.physb.2012.08.016.
18. Liang Dingshan, Zhao Cancan, Zhu Weiwei, Wei Pengbo, Jiang Feilong, Ren Fuzeng. Significantly enhanced wear resistance of an ultrafine-grained CrFeNi medium-entropy alloy at elevated temperatures. *Metallurgical and Materials Transactions A*, 2020, vol. 51, pp. 2834–2850. DOI: 10.1007/s11661-020-05755-8.
19. Zhang Hongbin, Chen Kang, Wang Zhongwei, Zhou Haiping, Gao Kuidong, Du Yichang, Su Yukuo. Microstructure and mechanical properties of novel Si-added CrFeNi medium-entropy alloy prepared via vacuum arc-melting. *Journal of Alloys and Compounds*, 2022, vol. 904, article number 164136. DOI: 10.1016/j.jallcom.2022.164136.
20. Peng Shibo, Lu Zheng, Yu Li. Control of microstructure and hardness of ODS-CrFeNi MEAs by Y_2O_3/Zr addition. *Materials Characterization*, 2022, vol. 186, article number 111816. DOI: 10.1016/j.matchar.2022.111816.
21. Makarov A.V., Soboleva N.N., Malygina I.Yu. Role of the strengthening phases in abrasive wear resistance of laser-clad NiCrBSi coatings. *Journal of Friction and Wear*, 2017, vol. 38, no. 4, pp. 272–278. DOI: 10.3103/S1068366617040080.

СПИСОК ЛИТЕРАТУРЫ

1. Cantor B., Chang I.T.H., Knight P., Vincent A.J.B. Microstructural development in equiatomic multicomponent alloys // Materials Science and Engineering: A. 2004. Vol. 375-377. P. 213–218. DOI: 10.1016/j.msea.2003.10.257.
2. Yeh Jien-Wei, Lin Su-Jien, Chin Tsung-Shune, Gan Jon-Yiew, Chen Swe-Kai, Shun Tao-Tsung, Tsau Chung-Huei, Chou Shou-Yi. Formation of simple crystal structures in Cu–Co–Ni–Cr–Al–Fe–Ti–V alloys with multiprincipal metallic elements // Metallurgical and Materials Transactions A. 2004. Vol. 35. P. 2533–2536. DOI: 10.1007/s11661-006-0234-4.
3. Zhang Yong, Zuo Ting Ting, Tang Zhi, Gao M.C., Dahmen K.A., Liaw P.K., Lu Zhao Ping. Microstructures and properties of high-entropy alloys // Progress in Materials Science. 2014. Vol. 61. P. 1–93. DOI: 10.1016/j.pmatsci.2013.10.001.
4. Butler T.M., Weaver M.L. Influence of annealing on the microstructures and oxidation behaviors of $Al_8(CoCrFeNi)_{92}$, $Al_{15}(CoCrFeNi)_{85}$, and $Al_{30}(CoCrFeNi)_{70}$ high-entropy alloys // Metals. 2016. Vol. 6. № 9. Article number 222. DOI: 10.3390/met6090222.
5. Daoud H.M., Manzoni A.M., Völkl R., Wanderka N., Glatzel U. Oxidation behavior of $Al_8Co_{17}Cr_{17}Cu_8Fe_{17}Ni_{33}$, $Al_{23}Co_{15}Cr_{23}Cu_8Fe_{15}Ni_{15}$, and $Al_{17}Co_{17}Cr_{17}Cu_{17}Fe_{17}Ni_{17}$ compositionally complex alloys (high-entropy alloys) at elevated temperatures in air // Advanced Engineering Materials. 2015. Vol. 17. № 8. P. 1134–1141. DOI: 10.1002/adem.201500179.
6. Gludovatz B., Hohenwarter A., Thurston K.V.S., Bei Hongbin, Wu Zhenggang, George E.P., Ritchie R.O. Exceptional damage-tolerance of a medium-entropy alloy CrCoNi at cryogenic temperatures // Nature Communications. 2016. Vol. 7. Article number 10602. DOI: 10.1038/ncomms10602.
7. Arif Z.U., Khalid M.Y., Rashid A.A., Rehman E.U., Atif M. Laser deposition of high-entropy alloys: A comprehensive review // Optics & Laser Technology. 2022. Vol. 145. Article number 107447. DOI: 10.1016/j.optlastec.2021.107447.
8. Xiang Kang, Chai Linjiang, Wang Yueyuan, Wang Hao, Guo Ning, Ma Yanlong, Murty K.L. Microstructural characteristics and hardness of CoNiTi medium-entropy alloy coating on pure Ti substrate prepared by pulsed laser cladding // Journal of Alloys and Compounds. 2020. Vol. 849. Article number 156704. DOI: 10.1016/j.jallcom.2020.156704.
9. Geng Yanfei, Konovalov S.V., Chen Xizhang. Research status and application of the high-entropy and traditional alloys fabricated via the laser cladding // Progress in Physics of Metals. 2020. Vol. 21. № 1. P. 26–45. DOI: 10.15407/ufm.21.01.026.
10. Juan Yongfei, Zhang Jiao, Dai Yongbing, Dong Qing, Han Yanfeng. Designing rules of laser-clad high-entropy alloy coatings with simple solid solution phases // Acta Metallurgica Sinica (English Letters). 2020. Vol. 33. P. 1064–1076. DOI: 10.1007/s40195-020-01040-0.
11. Chen Zhao, Wen Xiaoli, Wang Weili, Lin Xin, Yang Haiou, Jiang Ze, Chen Lianyang, Wu Haibin, Li Wenhui, Li Nan. Engineering fine grains, dislocations and precipitates for enhancing the strength of TiB_2-modified CoCrFeMnNi high-entropy alloy using Laser Powder Bed Fusion // Journal of Materials Research and Technology. 2023. Vol. 26. P. 1198–1213. DOI: 10.1016/j.jmrt.2023.07.244.
12. He Junyang, Makineni S.K., Lu Wenjun, Shang Yuanyuan, Lu Zhaoping, Li Zhiming, Gault B. On the formation of hierarchical microstructure in a Mo-doped NiCoCr medium-entropy alloy with enhanced strength-ductility synergy // Scripta Materialia. 2020. Vol. 175. P. 1–6. DOI: 10.1016/j.scriptamat.2019.08.036.
13. Ren Mengfei, Li Ruifen, Zhang Xiaoqiang, Gu Jiayang, Jiao Chen. Effect of WC particles preparation method on microstructure and properties of laser cladded Ni60-WC coatings // Journal of Materials Research and Technology. 2023. Vol. 22. P. 605–616. DOI: 10.1016/j.jmrt.2022.11.120.
14. Cao Qizheng, Fan Li, Chen Haiyan, Hou Yue, Dong Lihua, Ni Zhiwei. Wear behavior of laser cladded WC-reinforced Ni-based coatings under low temperature // Tribology International. 2022. Vol. 176. Article number 107939. DOI: 10.1016/j.triboint.2022.107939.
15. Sabzi M., Dezfuli S.M., Mirsaeedghazi S.M. The effect of pulse-reverse electroplating bath temperature on the wear/corrosion response of Ni-Co/tungsten carbide nanocomposite coating during layer deposition // Ceramics International. 2018. Vol. 44. № 16. P. 19492–19504. DOI: 10.1016/j.ceramint.2018.07.189.
16. Dash T., Nayak B.B. Preparation of multi-phase composite of tungsten carbide, tungsten boride and carbon by arc plasma melting: characterization of melt-cast product // Ceramics International. 2016. Vol. 42. № 1-A. P. 445–459. DOI: 10.1016/j.ceramint.2015.08.129.

17. Chen Hai-Hua, Bi Yan, Cheng Yan, Ji Guangfu, Peng Fang, Hu Yan-Fei. Structural and thermodynamic properties of WB at high pressure and high temperature // Physica B: Condensed Matter. 2012. Vol. 407. № 24. P. 4760–4764. DOI: 10.1016/j.physb.2012.08.016.
18. Liang Dingshan, Zhao Cancan, Zhu Weiwei, Wei Pengbo, Jiang Feilong, Ren Fuzeng. Significantly enhanced wear resistance of an ultrafine-grained CrFeNi medium-entropy alloy at elevated temperatures // Metallurgical and Materials Transactions A. 2020. Vol. 51. P. 2834–2850. DOI: 10.1007/s11661-020-05755-8.
19. Zhang Hongbin, Chen Kang, Wang Zhongwei, Zhou Haiping, Gao Kuidong, Du Yichang, Su Yukuo. Microstructure and mechanical properties of novel Si-added CrFeNi medium-entropy alloy prepared via vacuum arc-melting // Journal of Alloys and Compounds. 2022. Vol. 904. Article number 164136. DOI: 10.1016/j.jallcom.2022.164136.
20. Peng Shibo, Lu Zheng, Yu Li. Control of microstructure and hardness of ODS-CrFeNi MEAs by Y_2O_3/Zr addition // Materials Characterization. 2022. Vol. 186. Article number 111816. DOI: 10.1016/j.matchar.2022.111816.
21. Makarov A.V., Soboleva N.N., Malygina I.Yu. Role of the strengthening phases in abrasive wear resistance of laser-clad NiCrBSi coatings // Journal of Friction and Wear. 2017. Vol. 38. № 4. P. 272–278. DOI: 10.3103/S1068366617040080.

Влияние добавок карбида и борида вольфрама на структуру и микротвердость эквиатомного CrFeNi-покрытия, сформированного короткоимпульсной лазерной наплавкой

© 2024

Степченков Александр Константинович*[1,4], младший научный сотрудник
Макаров Алексей Викторович[1,5], доктор технических наук, член-корреспондент РАН, заведующий отделом материаловедения и лабораторией механических свойств
Волкова Елена Георгиевна[1,6], кандидат физико-математических наук, старший научный сотрудник
Эстемирова Светлана Хусаиновна[2,7], кандидат химических наук, старший научный сотрудник
Харанжевский Евгений Викторович[3,8], доктор технических наук, профессор, заведующий лабораторией физики и химии материалов

[1]*Институт физики металлов имени М.Н. Михеева Уральского отделения РАН, Екатеринбург (Россия)*
[2]*Институт металлургии Уральского отделения РАН, Екатеринбург (Россия)*
[3]*Удмуртский государственный университет, Ижевск (Россия)*

***E-mail: stepchenkov@imp.uran.ru, alexander.stepchenkov@gmail.com**

[4]ORCID: https://orcid.org/0000-0001-9431-0170
[5]ORCID: https://orcid.org/0000-0002-2228-0643
[6]ORCID: https://orcid.org/0000-0003-4958-3027
[7]ORCID: https://orcid.org/0000-0001-7039-1420
[8]ORCID: https://orcid.org/0000-0002-1525-2169

Поступила в редакцию 27.06.2023 *Принята к публикации 30.01.2024*

Аннотация: Покрытие на основе однофазного среднеэнтропийного сплава CrFeNi с гранецентрированной кубической (ГЦК) структурой обладает хорошей пластичностью, относительно высокими антикоррозионными свойствами, низкой стоимостью, но недостаточной прочностью для его широкого применения. Предполагается, что добавление упрочняющих частиц в виде карбидов и боридов вольфрама в эквиатомное CrFeNi-покрытие приведет к повышению его механических свойств. В работе изучено влияние добавок карбида и борида вольфрама на структуру и микротвердость эквиатомного CrFeNi-покрытия. Формирование покрытий осуществлялось путем послойного короткоимпульсного лазерного оплавления предварительно нанесенного порошка на многофункциональной лазерной установке, оснащенной твердотельным лазером с ламповой накачкой на основе кристалла Nd:YAG. Изменение фазового состава при добавлении упрочняющих частиц выявлялось с помощью методов рентгеновского дифракционного анализа и просвечивающей электронной микроскопии (ПЭМ). Оба метода подтвердили выделение в наплавленных покрытиях карбида хрома $Cr_{23}C_6$. Фотографии, полученные при помощи ПЭМ, указывают на то, что выделяемая фаза распределена по границам зерен γ-твердого раствора. Установлено, что добавление 6 мас. % WC и 3 мас. % WB повышает уровень микротвердости CrFeNi-покрытия на 26 % (с 340±6 до 430±12 HV 0,025) вследствие наличия в структуре частиц $Cr_{23}C_6$, WC и возможных микроискажений кристаллической решетки γ-фазы в результате легирования атомами вольфрама, высвободившимися при растворении боридов и карбидов вольфрама в процессе высокотемпературного короткоимпульсного лазерного нагрева.

Ключевые слова: CrFeNi-покрытие; среднеэнтропийные сплавы; карбиды/бориды вольфрама; короткоимпульсная лазерная наплавка; эквиатомные покрытия; микротвердость.

Благодарности: Работа выполнена в рамках государственного задания ИФМ УрО РАН по теме «Структура» № 122021000033-2. Исследования проводились с использованием оборудования отделов электронной микроскопии и механических испытаний ЦКП «Испытательный центр нанотехнологий и перспективных материалов» ИФМ УрО РАН.

А.К. Степченков благодарит Институт физики металлов имени М.Н. Михеева за поддержку работы по государственному заданию ИФМ УрО РАН по теме «Структура» № 122021000033-2, которая выполнялась в рамках молодежного проекта ИФМ УрО РАН № 22-13/мол.

Статья подготовлена по материалам докладов участников XI Международной школы «Физическое материаловедение» (ШФМ-2023), Тольятти, 11–15 сентября 2023 года.

Для цитирования: Степченков А.К., Макаров А.В., Волкова Е.Г., Эстемирова С.Х., Харанжевский Е.В. Влияние добавок карбида и борида вольфрама на структуру и микротвердость эквиатомного CrFeNi-покрытия, сформированного короткоимпульсной лазерной наплавкой // Frontier Materials & Technologies. 2024. № 1. С. 83–94. DOI: 10.18323/2782-4039-2024-1-67-8.